Mechanics

Shear Stresses in the Indirect Test of Tensile Strength of Rocks and other Hard Materials

Levan Japaridze

Academy Member, G. Tsulukidze Mining Institute, Tbilisi, Georgia

ABSTRACT. In the paper some theoretical and practical problems of the indirect test of tensile strength of materials, known as the Brazilian method are considered. The contact width, corresponding loading angle, and elliptical stresses obtained through solution of the contact problems are used as boundary conditions for cylindrical specimen. The problem of the theory of elasticity for a cylinder is solved using Muskhelishvili's method. Numerical examples are solved using MATLAB to demonstrate the influence of deformability, curvature of the specimen and platens on the distribution of the normal contact stresses as well as on the tensile and compressive stresses acting across the loaded diameter. In the paper firstly is given a quantitative assessment of principal normal and shearing stresses in diametrical and nearby chordal sections of a cylindrical specimen, where they can reach critical magnitudes and create initial local tensile-shear cracks long before the tensile stresses reach their limit in the center of the disk. In such cases the most likely place of splitting a disk in the Brazilian test is not diametrical, but is along chordal surfaces, which occur on border lines of the loading area. © 2016 Bull. Georg. Natl. Acad. Sci.

Key words: Brazilian test method; tensile strength; shear stresses; tensile-shear cracks.

The Brazilian test, developed by Carneiro and Barcellos [1], found widespread application because of its practical convenience. The International Society for Rock Mechanics (ISRM) [2] officially suggested the indirect method for determining the tensile strength of rock materials. The standard test method can be followed according to American Society for Testing and Materials (ASTM) [3] for different kinds of anisotropy and homogeneity of testing rocks, concretes, glass, and many other brittle and not quite brittle materials (e.g. nuclear wastes (ASTM C1144-89) [4], asphalt concrete etc.). The European standard for testing the tensile strength of concrete specimens was approved by the European Committee for Standardization (BS EN 12390-6: 2000) [5].

The history of development and widespread practical application of the Brazilian test in rock mechanics was reviewed and investigated most recently by numerous scientists, [6-8]. Ever since the development of the Brazilian test method scientists were interested in the questions:

• Why are samples often not split along the loading diameter, as to the basic idea of the Brazilian test, but at some distance away from it?

• How and why does Brazilian test overestimate the tensile strength of materials [6,9]?

A number of scholars paid attention to these problems shortly after the popularization of the Brazilian test method, e.g. Hudson [10,11], Mellor and Hawkes [12], Hooper [13], Wijk [14], Hondros [15], Chen et al. [16], Lavrov and Vervoort [17], Marion and Johnstone [18], Procopio et al. [19], Jonsen and Haggblad [20], Markides and Kourkoulis [21], Japaridze [9,22,23] and others suggested different analytical and numerical solutions and improved schemes, generalized for different kinds of anisotropy and homogeneity of testing rocks, concretes and other materials.

In the vast majority of these studies much attention was placed on the components of tensile and compressive normal stresses, or deformations in the diametrical section of the disk specimen. It is assumed that tensile stresses are mainly responsible for splitting a sample. The primary cracks always are tensile cracks appearing in the center of a disk, and shear cracks, if they generally appear on the disk periphery, as a rule, are secondary ones. The role of the deviatoric shear stresses in the chordal sections, in the formation of cracks in the sample long has been seen only qualitatively, although, as is known, the deviatoric stresses control the distortion, and many of the criteria for failure are concerned primarily with distortion. Consequently, some of the above mentioned questions, especially concerning the mode of failure of specimens in the Brazilian test, remain open for solution. Different results of the experiments and various opinions and explanations of these results continue to exist today.

A sufficiently full description of this diversity is given by Li and Wong [6]. Typical interpretations of the different investigators concerning the crack initiation and propagation may be grouped in the following way:

1. The failure of the Brazilian disc begins as an extension fracture in the center (interior) of the disk and then propagates to the top and bottom surfaces [24-27]. Cracks will occur if the maximum tensile stress exceeds the tensile strength.

2. In some laboratory Brazilian tests the crack initiation points was observed to be located away from the center of the test disc [7]. In addition, the stress concentration near the loading platen occasionally leads to an early shear failure fracture in the rock [7,10,26,28].

3. The crack initiation point of the Brazilian test may be located near the loading point [6,8,9].

Influence of mechanical parameters of the sample material and loading device on the rupture character of the cylindrical specimens and on the results of Indirect Tensile Splitting "Brazilian" test, still presents the subject of an experimental study for scientists.

This paper analyzes the fields of the normal stresses and of the shear stresses, derived in two dimensional closed form solution adopting the complex potentials method of N.Muskhelishvili [29].

Experimental Background

Influence of mechanical parameters of the sample material and loading device on the rupture character of the cylindrical specimens and on the results of Indirect Tensile Splitting "Brazilian" Test still presents the subject of an experimental study for scientists. From the numerous experimental investigations and practical applications of the Brazilian test for rocks and other hard materials some of them are considered below.

The Standard Test Method for Splitting Tensile Strength of Intact Rock Core (ASTM) [3] was used by Daemen [7] for Yucca Mountain Tuffs (Fig. 1, a, b), by Basu [30] for sandstone and granite (Fig. 1, c, d). Similar forms of cylindrical specimens rupture have been reported by Rocco et al. [31] for concretes, Iglesias, et al. [32] for ceramics, Johnsen, et al. [20] for compacted powders, and others.

It should be kept in mind, that in the most part of these works diametrical or nearly diametrical fractures are categorized as primary, and the fractures, which deviate from the center too much are considered as second-

(a)   (b)   (c)   (d)
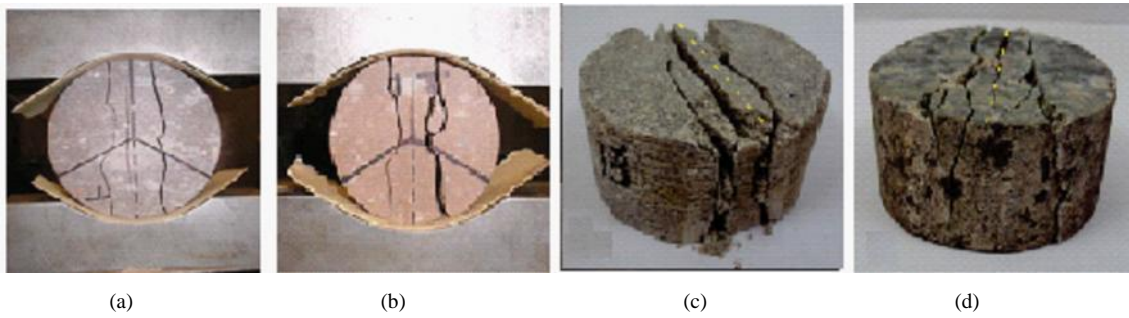
Fig. 1. Examples of chordal fracture in Brazilian test of Yucca Mountain Tuffs (a,b)
(From Daemen, et al. [7], sandstone (c) and granite (d) specimens
(From Basu, et al. [30]).

ary ones. However, as it was noted already by Mellor and Hawkes [12], even fastax photography could not identify the origin of the sequence and there is no experimental evidence that the diameter of the sloping curve of the shape of the cracks is always experimental technical error, or the result of sample heterogeneity. To date there uncertainty often remains for Brazilian tests as to whether cracks begin from the contact surface of the sample or from the center.

Theoretical Prerequisites

Typical schematics of the devices of Suggested Method for Determining Indirect Tensile Strength by the Brazilian test according to International Society for Rock Mechanics (ISRM) [2], Standard Test Method for Splitting Tensile Strength of Intact Rock Core Specimen of American Society for Testing and Materials (ASTM) [3,4] and the European Standard EN 12390-6:2000 has the status of British Standard BS EN 12390-6:2000 [5], are represented in Fig.2.

In the long practice of the application of the Brazilian test in the ASTM method as well as ISRM and other standardized methods, the splitting tensile strength $\dagger_t$ shell be calculated as follows:

$$\dagger_t = \frac{P}{f\, R_1 L} \tag{1}$$

were - P – maximum applied load indicated by the testing machine; L and R_1 – thickness and radius of the specimen.

According to (1) it is assumed that the principal tensile stresses are distributed uniformly along the vertical diameter $\left(-R_1 \le y \le R_1\right)$ and thees tensile stresses are responsible for failure of the specimen in the Brazilian test. More refined analytic solutions for standardized Brazil test schemes are given by Kourkoulis and Markides [33] and Japaridze [9,22,23]. In their studies a cylindrical specimen with radius R_1 , length L and the loading jaws with radius of the contact faces R_2 compressed (Fig. 3) by forces P, touch each other on the surfaces with angle width $2_{\#0}$.

According to the derivations of the contact tasks of the theory of elasticity [34,35], the half-width of the contact surface - a is given by:

$$a = \sqrt{\frac{2 P R_1 K}{f\, L\left(1 - R_1/R_2\right)}\left(\frac{|_1 + 1}{4\sim_1} + \frac{|_2 + 1}{4\sim_2}\right)}, \tag{2}$$

where: "Muskhelishvili's coefficient" is defined as $|_1 = (3 - 4\mathbb{E}_1),\quad |_2 = (3 - 4\mathbb{E}_2),$ for plane strain (when,
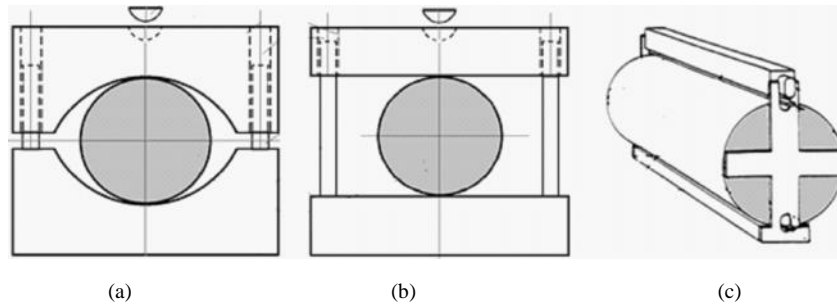
Fig. 2. The schemes of apparatus of ISRM (a), of ASTM (b) and BS EN (c) Standard Test Methods for Splitting Tensile Strength of Intact Rock Core Specimen.
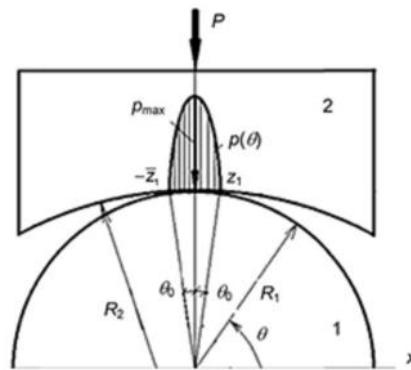
Fig. 3. Compression of a cylindrical specimen between curved jaws. z_1 and $-\bar{z}_1$ are the boundary points of the contact surface.

for example, in the Brazilian test the thickness of the disk is more than the radius, i.e. $L > R_1$) and $\chi_1 = (3 - \epsilon_1) / (1 + \epsilon_1)$, $\chi_2 = (3 - \epsilon_2) / (1 + \epsilon_2)$, for plane stress, when $L < R_1$; shear modulus $\mu_1 = E_1 / 2(1 + \epsilon_1)$, $\mu_2 = E_2 / 2(1 + \epsilon_2)$, ϵ_1, E_1 and ϵ_2, E_2 are Poisson's ratios and elasticity module of contacted bodies, respectively.

In equation (2) R_2 is positive when the centers of the curvature of the specimen and the jaws are on the same side (as shown in Fig. 1), and it is negative when the centers are on different sides from the contact line $y = \pm R_1$.

If the frictional contact stresses between the specimen and platens are neglected because of their smallness [34-36], the contact pressure in the polar coordinates will be:

$$p(\theta) = \frac{2P}{f a^2 L} \sqrt{a^2 - R_1^2 \cos^2 \theta} \; , \tag{3}$$

where $(f / 2 - \theta_0) \le \theta \le (f / 2 + \theta_0)$; $(3f / 2 - \theta_0) \le \theta \le (3f / 2 + \theta_0)$, $\theta_0 = \arcsin(a / R_1)$.

It is easy to prove that (3) represents the equation of an ellipse with the small semi-axis as a half-width of the contact surface (2) and the big semi-axis $2P / f aL$ presenting maximum contact stress $p_{\max}$ at the points $\theta = f / 2$ and $\theta = 3f / 2$. Using series expansion, equation (3) can be expressed in the complex formulation as follows:

$$p(\theta) = \frac{4P}{f (z_1 + \bar{z}_1)} \left[1 - \frac{R_1^2}{(z_1 + \bar{z}_1)^2} - \frac{z^2 + \bar{z}^2}{2(z_1 + \bar{z}_1)^2} \right], \tag{4}$$

where $z = x + iy = re^{i\theta}$, $z_1 = R_1 e^{i\theta_0}$, $\overline{z}_1 = R_1 e^{-i\theta_0}$, $\theta_0 = \arccos(a/R_1)$, $z_1 + \overline{z}_1 = 2a$. Points z and z_1 on the complex plane $\zeta = z/R_1$ correspond to the points $\tau = e^{i\theta}$, and $\tau_1 = e^{i\theta_0}$. Consequently, if to use the correction for the equivalence of sum vector of contact pressure to the external load P:

$$A = \frac{P}{4.4 f\, a^3}\left(8a^2 - 2R_1^2\right) \quad \text{and} \quad B = -\frac{P}{4.4 f\, a^3}, \tag{5}$$

boundary conditions according to (4), (5) and [29] can be written as:

$$\Phi(\tau) + \overline{\Phi(\tau)} - \tau\Phi'(\tau) - \tau^2\Psi(\tau) = A + B\left(\tau^2 + \overline{\tau}^2\right). \tag{6}$$

where $\Phi(\tau)$ and $\Psi(\tau)$ are the sought functions of complex potentials on the plane $\tau = e^{i\theta}$, $\overline{\Phi(\tau)}$ is a conjugate and $\Phi'(\tau)$ is a derivation of $\Phi(\tau)$. Corresponding analytic functions of the complex potentials obtained in [22,23] are given by:

$$\Phi(z) = \frac{1}{2 f i}\left[\left(A - B\frac{z^2}{R_1^2} - \frac{BR_1^2}{z^2}\right)\ln\frac{\overline{z}_1^2 - z^2}{z_1^2 - z^2} - \left(\frac{A}{2} - \frac{BR_1^2}{z^2}\right)\ln\frac{\overline{z}_1^2}{z_1^2}\right]; \tag{7}$$

$$\Psi(z) = \frac{1}{f i}\left[\left(A - B\frac{z^2}{R_1^2} - \frac{BR_1^2}{z^2}\right)\left(\frac{R_1^2}{\overline{z}_1^2 - z^2} - \frac{R_1^2}{z_1^2 - z^2}\right) + \left(B - \frac{BR_1^4}{z^4}\right)\ln\frac{\overline{z}_1^2 - z^2}{z_1^2 - z^2} + \frac{BR_1^4}{z^4}\ln\frac{\overline{z}_1^2}{z_1^2}\right]. \tag{8}$$

The combination of normal σ_x, σ_y and tangential τ_{xy} stress components in the disk section can be found by substituting these functions into the well-known formulas of Kolosov–Muskhelishvili [29] for a Cartesian reference system:

$$\begin{aligned} \sigma_x + \sigma_y &= 2\left[\Phi(z) + \overline{\Phi(z)}\right]; \\ \sigma_x - \sigma_y + 2i\tau_{xy} &= 2\left[\overline{z}\Phi'(z) + \Psi(z)\right]. \end{aligned} \tag{9}$$

The normal stresses along the loaded diameter $(x=0)$, obtained in this way are given in [22,23]. The normal: σ_x, σ_y and shear τ_{xy} stresses in the arbitrary point of a disk according to functions of the complex potentials (7),(8) and equations (9) are given by:

$$\left.\begin{aligned}\sigma_x \\ \sigma_y\end{aligned}\right\} = real\, \frac{B}{f i}\left[\begin{array}{l}\left(\dfrac{A}{B} - z^2 - \dfrac{R^4}{z^2}\right)\ln\dfrac{\overline{z}_1^2 - z^2}{z_1^2 - z^2} - \left(\dfrac{A}{2B} - \dfrac{R_1^4}{z^2}\right)\ln\dfrac{\overline{z}_1^2}{z_1^2} \mp \left(\dfrac{A}{B} - z^2 - \dfrac{R_1^4}{z^2}\right)\dfrac{\left(\overline{z}_1^2 - z_1^2\right)\left(\overline{z}z - R_1^2\right)}{\left(\overline{z}_1^2 - z^2\right)\left(z_1^2 - z^2\right)} \mp \\[2ex] \mp\left(\dfrac{R_1^4\overline{z}}{z^3} - z\overline{z} + R_1^2 - \dfrac{R_1^6}{z^4}\right)\ln\dfrac{\overline{z}_1^2 - z^2}{z_1^2 - z^2} \pm \left(\dfrac{R_1^4\overline{z}}{z^3} - \dfrac{R_1^6}{z^4}\right)\ln\dfrac{\overline{z}_1^2}{z_1^2}\end{array}\right]; \tag{10}$$

$$\tau_{xy} = imag\, \frac{B}{f i}\left[\begin{array}{l}\left(\dfrac{A}{B} - z^2 - \dfrac{R_1^4}{z^2}\right)\dfrac{\left(\overline{z}_1^2 - z_1^2\right)\left(\overline{z}z - R_1^2\right)}{\left(\overline{z}_1^2 - z^2\right)\left(z_1^2 - z^2\right)} + \left(\dfrac{R_1^4\overline{z}}{z^3} - z\overline{z} + R_1^2 - \dfrac{R_1^6}{z^4}\right)\ln\dfrac{\overline{z}_1^2 - z^2}{z_1^2 - z^2} - \\[2ex] -\left(\dfrac{R_1^4\overline{z}}{z^3} - \dfrac{R_1^6}{z^4}\right)\ln\dfrac{\overline{z}_1^2}{z_1^2}\end{array}\right]. \tag{11}$$

As the calculation will be implemented using MATLAB, to write cumbersome transformation for the separation of real and imaginary parts of eq. (10, 11) makes no sense. It will be done by MATLAB.

Discussion

Using the above mentioned analytic apparatus the numerical examples are calculated for the initial data close to Daemen's, et al. [7] experimental results: radius and thickness of disc specimen R_1 =3 cm, t=2.5 cm; radius of jaws curvature according to ISRM R_2 =1.5 R_1 =4.5 cm; elasticity modulus and Poisson's ratio of disc material: E_1 =15 GPa, ϵ_1 =0.19; elasticity modulus and Poisson's ratio of the jaws material: E_2 =210 GPa, ϵ_2 =0.3; maximum applied load P=50 kN.

For these initial data the tensile strength of given samples according to eq. (1), $\dagger_t$ = 21.22 MPa, the width of contact pressure distribution arcs and the appropriate central angle, calculated from (2), $2a$=0.78 cm and $2_{n\,0} \approx 14°$. The components of normal $\dagger_x$, $\dagger_y$ and shearing $\ddagger_{xy}$ stresses in diametrical section (x=0) and in nearby chordal sections at a distance from the disk centre equal to half width (x=0.5a) and to the width (x=a) of contact interface are computed by MATLAB according to equations (10), (11).

Graphical representations of these stresses, normalized against Hertzian tensile stress (1), i.e. appropriate stress concentration factors of tension $T = \dagger_x f R_1 L / P$, compression $C = \dagger_y f R_1 L / P$ and shearing $S = \ddagger_{xy} f R_1 L / P$ in the Cartesian coordinates are given in Fig.4. Numerical extremal values of these stress concentration factors at the disk diameter (x/a=0) and nearby chordal sections (x/a =1) for the applied load P=50 kN, radius and thickness of disc specimen R_1 =3 cm, t=2.5 cm; radius of jaws curvature R_2 = 1.5R_1; $R_2 = \infty$; modulus of deformation E_1 =10 ,15, 20 GPa and Poisson's ratio of disc material ϵ_1 =0.19; elasticity modulus and Poisson's ratio of the jaws material: E_2 =300 GPa, ϵ_2 =0.3, are given in Table 1.

Fig. 4 and Table 1 illustrate: The maximum tensile stress concentration factor in the center of a disk for the given initial parameters varies in limits 0.89-0.91, i.e., intensity of tensile stress here differs by 9-11% from the same, calculated from Hertz's eq.(1), which is now applied in the standardized methods. This difference is the first factor of overestimation of tensile strength in Brazilian test. Value of this difference increases with the
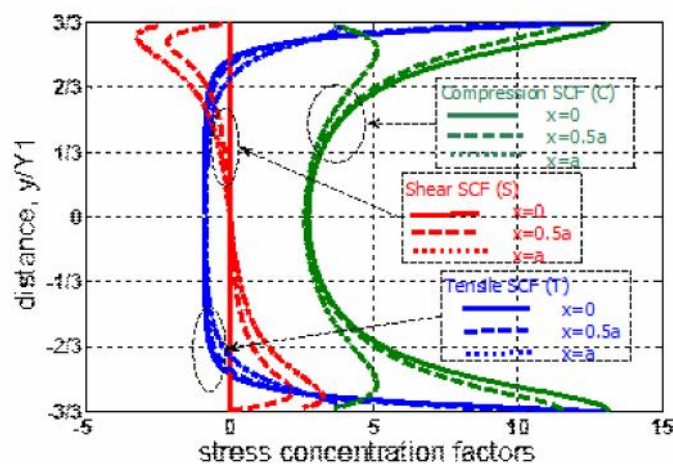
Fig. 4. Principal normal tensile (T), compressive (C) and shear (S) stress concentration factors (SCF), on the vertical diameter (x=0; 0<y/R_1< 1), and on the nearby chordal sections (x=0.5a) and (x=a).

Table 1. Extremal values of stress concentration factors: T,C,S at the disk diameter (x/a=0) and nearby chordal sections (x/a =1) for the: applied load P=50 kN; radius and thickness of disc specimen R_1=3 cm, t=2.5 cm; radius of jaws curvature R_2=1.5R_1= and R_2=¿; modulus of deformation E_1 and Poisson's ratio of disc material ϵ_1=0.19; elasticity modulus and Poisson's ratio of the jaws material: E_2=300 GPa, ϵ_2=0.3

E_1	10 (Gpa)				15 GPa				20 GPa			
R_1/R_2	0.67 (ISRM)		0 (ASTM)		0.67 (ISRM)		0 (ASTM)		0.67 (ISRM)		0 (ASTM)	
a/R_1	0.159		0.092		0.131		0.076		0.114		0.066	
$2_{,0}$ (°)	18.3		10.5		15.04		8.67		13.1		7.56	
x/a	0	1	0	1	0	1	0	1	0	1	0	1
T	0.890	0.806	0.905	0.875	0.897	0.839	0.908	0.887	0.901	0.856	0.909	0.893
C	2.722	2.549	2.733	2.672	2.727	2.607	2.735	2.693	2.730	2.638	2.735	2.704
S	0.0	2.630	0.0	4.625	0.0	3.221	0.0	5.637	0.0	3.708	0.0	6.450

decrease of modulus of deformation of specimen and will be bigger for curved jaws (ISRM) in comparison to both: plane plates (ASTM) and/or sharp indenters.

The intensity of the tensile stress decreases with the distance from the center and in some points $y = \pm y_0$, the tensile stress equal to zero. Over these points the sign of the normal stresses changes and compressive stress rapidly increases approaching to the boundary [23]. These points are closer to the center and accordingly, the diametrical part of action of compressive stresses is bigger as the rigidity of the specimen-platen is lower and the contact interface is wider. The action of high intensity compressive stresses in the external parts of the loading diameter will somewhat impede the spreading of the diametrical tension crack from the central part of a disk. This may be the second factor of overestimation of tensile strength in the Brazilian test.

Principal normal $\dagger_x$, $\dagger_y$ in the internal part (x=0, $y = \pm y_0$) of the disk diameter and in nearby chordal sections (x/a =0 $\div$1) differ little from each other, but this difference increases very significantly in the peripheral parts of these sections. The shear stresses also grow rapidly and near the contour (x=a, $y / R_1 \approx 0.9$) of the disk, shear stress concentration factor S=2.6$\div$6.5 . It means that for given typical initial conditions (E_1 =10$\div$20 GPa) maximum shear stress 3.25$\div$7.3 times more than maximum tensile stress.

Such large shear stress on the edges of the loading surface confirm that non-elastic deformations, plastic bands and possibly primary local cracks can appear on the front line of the loading interface long before tensile stresses reach their limit in the center of a disk. At the same time widening of the loading interface leads to the lateral movement of the contact edge, where the maximum shear stress occur. These results in the so-called "atypical" fractures (Fig.1), appearance of which usually is considered as indication of an invalid experiment. This kind of failure mode was observed in experiments and is described in publications [7,12,20,30,32].

At the same time the development of the oncoming cracks due to shear stresses in the chordal sections can complete the splitting of the disk. Such "tensile-shear" kind of the failure mode has been observed in experiments and is qualitatively described in the publications and more recently [6,8].

Analytical assessments and tests show that it is very difficult to avoid non-elastic deformation on a disk-jaw contact without loss of test accuracy. Application of the curved jaws or false platens of low yield point metal, or cardboard "platen cushions" cannot completely exclude local inelastic deformation on the loading surface. The latter will cause widening of the contact width, lowering of the peak contact pressure and

reducing of the stress concentrations factors. Plastic deformations on a thin of the contact rim practically will not influence the tensile stresses on a large internal parts both of the loaded diameter and nearby choral sections. But as a result of contact widening, very large shear stresses in the external parts of these choral planes appear, whereas in the internal part of these chordal planes tensile stresses act, that differ little from the stress in the loaded diameter. So in such cases the most likely place of splitting a cylindrical disk in the Brazilian test becomes the chordal planes and the cleavage occur due to shearing, but not by spliting.

Conclusions

1. In this paper attention is paid to the deviatoric shear stresses, tensile and compressive normal stresses in the nearby off-diametrical chordal sections, and to their role in the formation of cracks in the sample. The study underlines this problem on the basic of the results of experimental and analytic investigations and presents the quantitative assessment of principal normal and shearing stresses in diametrical as well as nearby chordal sections of a cylindrical specimen, where they can reach critical intensity and create initial local tensile-shear cracks .

2. Analytic solutions are derived in two dimensional closed form solution, applying the complex potentials method. The results are compared with those of an experimental study of mechanical behavior of rocks and other hard isotropic, homogenous materials.

3. The maximal tensile stress concentration factor in disk center for the given initial parameters differs from the same, calculated from Hertz's equation, which is now is applied in the standardized methods. This difference is first factor of overestimation of tensile strength in Brazilian test. Value of this difference increases with the decrease of modulus of deformation of specimen and will be bigger for curved jaws (ISRM) in comparison to both: plane plates (ASTM) or sharp indenters.

4. The action of high intensity compressive stresses in the external parts of the loading diameter somewhat impedes the spreading of the diametrical tension crack from the central part of a disk. This may be the second factor of overestimation of tensile strength in Brazilian test.

5. The intensity of shear stresses in peripheral parts of chordal planes grows rapidly, and near the contour ($x=a$, $y/R_1 \approx 0.9$) of a disk, shear stress concentration factor S=2.6÷6.5 . It mean that for given typical initial conditions (E_1 =10÷20 GPa), maximum shear stresses 3.25÷7.3 times more, than the maximum tensile stress in a disk center. This can result in non-elastic deformations, plastic bands and the appearance of primary local cracks in the front region of the loading interface, and at last so-called "atypical" fractures long before the tensile stresses reach their limit in the center of a disk.

6. The most likely place of splitting cylindrical disk in Brazilian test is not always diametrical, but often is along the chordal surfaces, which occur on border lines of the loading area. These planes come nearer to the center with narrowing of the contact area and theoretically will coincide with the diametrical plane in the case of linear loading. Practically this is more possible, if one uses sharp indentors, small-diameter steel rods on the contacts, or at least the plane rigid platens (ASTM Standardized method), the use of which therewith relieves the necessity to prepare additional pairs of jaws for specimens with different diameter.

Acknowledgements

მექანიკა

მხები ძაბვები ქანების და სხვა მყარი მასალების გაჭიმვაზე სიმტკიცის არაპირდაპირი გამოცდისას

ლ. ჯაფარიძე

აკადმიის წევრი, გ.წულუკიძის სამთო ინსტიტუტი, თბილისი, საქართველო

სტატიაში გაანალიზებულია მყარი მასალის ცილინდრულ ნიმუშში ძაბვების განაწილების სურათი მისი გაჭიმვაზე სიმტკიცის არაპირდაპირი, ე.წ. ბრაზილიური მეთოდით დადგენისას. მეთოდი საერთაშორისო საზოგადოებამ ქანების მექანიკაში (ISRM, 1988), ამერიკის კავშირმა მასალების გამოცდაში (ASTM, 2008) და ევროპის სტანდარტიზაციის კომიტეტმა (BS EN 12390-6: 2000) ოფიციალურად ცნეს სტანდარტულ მეთოდად ქანების, ბეტონების, მინების და სხვა მყარი მასალების გაჭიმვის სიმტკიცის დასადგენად. ამ მეტად საჭირო მეთოდის დასახუსტებლად ჩატარებულ კვლევებში მეცნიერთა ყურადღება დღემდე ექცევა მხოლოდ გამჭიმავ ნორმალურ მთავარ ძაბვებს ცილინდრული ნიმუშის დიამეტრულ კვეთში. ამ სამუშაოში პირველად წარმოდგენილია რაოდენობრივი შეფასება მთავარი ნორმალური და დევიატორული მხები ძაბვებისა, როგორც დიამეტრულ, ისე მის პარალელურ ქორდალურ სიბრტყეებზე, სადაც მათ შეიძლება მიაღწიონ მასალის სიმტკიცის ზღვარს უფრო ადრე, ვიდრე დისკოს ცენტრში, რამაც შეიძლება გამოიწვიოს ცდომილება ამ მეთოდის გამოყენებისას. ამოცანა განხილულია როგორც ერთგვაროვანი, იზოტროპული, დრეკადი ცილინდრული დისკოს ბრტყელი დაძაბული მდგომარეობა, ან ბრტყელი დეფორმაცია. ანალიზური ამოხსნები მიღებულია ნ.მუსხელიშვილის კომპლექსური პოტენციალების მეთოდის გამოყენებით. რიცხვითი მაგალითები დათვლილია კომპიუტერული პროგრამა MATLAB-ის საშუალებით. შედეგები შედარებულია ექსპერიმენტულ მასალასთან.

REFERENCES:

1. *Carneiro F., Barcellos A.* (1953) RILEM Bull. 13:99–125.
2. ISRM (1981) Suggested Methods. Rock Characterization Testing and Monitoring, Suggested methods for determining tensile strength of rock materials. Pergamon Press, Oxford. Pp.119-121.
3. ASTM C1144 (1989) Standard Test Method for Splitting Tensile Strength for Brittle Nuclear Waste Forms, ASTM International, West Conshohocken, PA.
4. ASTM D 3967-08 (2008) Standard test method for splitting tensile strength of intact rock core specimens. ASTM International, West Conshohocken, USA.
5. BS EN 12390-6 (2000) British Standard.Testing hardened concrete . Part 6: Tensile splitting strength of test specimens.
6. *Li DY, Wong LNY* (2013) Rock Mechanics and Rock Engineering. 46(2): 269-87.
7. *Daemen JK, Ma LM., Zhao GH.* (2006) Final Technical Report for Task ORD-FY04e021. Reno, USA: Department of Mining Engineering, University of Nevada; http://digitalscholarship.unlv.edu/yucca mtn pubs/17.
8. *Ye Jianhong, F.Q.Wu., J.Z.Sun* (2009) International Journal of Rock Mechanics & Mining Sciences. 46: 568–576.

9. *L.A.Dzhaparidze* (1972) Journal of Mining Science (Translated from Russian). Springer International Publishing AG. 8, Issue 3: 331-334. http://link.springer.com/article/10.1007/BF02505722.

10. *Hudson JA.* (1969) International Journal of Rock Mechanics and Mining Sciences, 6(1):91–97. doi:10.1016/ 0148-9062(69)90029-1.

11. *Hudson JA, Brown ET., Rummel F.* (1972) International Journal of Rock Mechanics and Mining Sciences. **9**(2): 241–248. doi:10.1016/0148-9062(72)90025-3.

12. *Mellor M., Hawkes I.* (1971) Eng. Geol. 5: 173-225.

13. *Hooper J.A.* (1971) J. Mech. Phys. Solids, **19**, 4: 179–188.

14. *Wijk G.* (1978) International Journal of Rock Mechanics and Mining Sciences and Geomechanics Abstracts **15**(4):149e60.

15. *Hondros G.* (1959) Austral. J. Appl. Sci.10: 243–64.

16. *Chen CS., Pan E., Amadei B.* (1998) International Journal of Rock Mechanics and Mining Sciences. **35**(1): 43-61.

17. *Lavrov A., Vervoort A.* (2002) International Journal of Rock Mechanics and Mining Sciences. 39(2): 275e83.

18. *Marion RH., Johnstone JK.* (1977) American Ceramic Society Bulletin. 56(11): 998-1002.

19. *Procopio AT., Zavaliangos A., Cunniangham JC.* (2003) Journal of Materials Science. 38(17): 3629-39.

20. *Jonsen P. and Haggblad H.-A.* (2007) Inter. J. Solids and Structures. 44: 6398–6411.

21. *Markides CF., Kourkoulis SK.* (2016) J. Rock Mech. Geotech. Eng. 8: 127–146.

22. *Japaridze L.A.* (1971) Bulletin of the Academy of Sciences of the Georgian SSR. 62(3): 537e40.

23. *Japaridze L.A.* (2015) J. Rock Mech Geotech Eng; 7 (5): 509–518. http://www.sciencedirect.com/science/ article/pii/S1674775515000815.

24. *Yanagidani T., Sano O., Terada M., Ito I.* (1978) International Journal of Rock Mechanics and Mining Sciences Geomech. Abstr.; 15(5): 225–235. doi:10.1016/0148-9062(78)90955-5.

25. *Cai M., Kaiser PK.* (2004) International Journal of Rock Mechanics and Mining Sciences. 41: 2B 0301-06. doi:10.1016/j.ijrmms.2004.03.086.

26. *Van De Steen B., Vervoort A., Napier JAL.* (2005) Int. J. Fract. 131(1):35–52.

27. *Zhu WC., Tang CA.* (2006) International Journal of Rock Mechanics and Mining Sciences. 43(2):236–252. doi:10.1016/j.ijrmms. 2005.06.008.

28. *Fairhurst C.* (1964) International Journal of Rock Mechanics and Mining Sciences. 1(4):535–546. doi:10.1016/ 0148-9062(64)90060-9.

29. *Muskhelishvili N.I.* (1963) Some basic problems of the mathematical theory of elasticity. The 4th ed. Groningen, Netherlands: Noord hoff.

30. *Basu A., Mishra D. A., Roychowdhury K.* (2013) Bull. Eng. Geol. Environ. 72: 457–475. DOI 10.1007/s10064-013-0505-4.

31. *Rocco C., Guinea G., Planas J., Elices M.* (1999) ACI Materials Journal. 96: 52-60.

32. *Iglesias I., Acosta B., Yu R., Ruiz G., Aineto M., Acosta A.* (2011) Materials and Constructions. 61, 303: 417-429, ISSN: 0465-2746. doi: 10.3989/mc..55809, p.425.

33. *Kourkoulis S.K., Markides Ch.F., Chatzistergos P.E.* (2012) International Journal of Solids and Structures. 49: 959–972.

34. *Shtaerman P.* (1949) Contact tasks of the theory of elasticity. Moscow-Leningrad, USSR: Gostechizdat (in Russian).

35. *Timoshenko S.P. and Goodier J. N.* (1970) Theory of Elasticity, 3rd ed., McGr aw-Hill, New York.